

## Tracking of propagating turbulent flames and autoignition in enclosure

S.M. Frolov, V.S. Ivanov, V.A. Smetanyuk, B. Basara\*

*Department of Combustion and Explosion, Semenov Institute of Chemical Physics, Moscow, RUS  
Advanced Simulation Technologies, AVL List GmbH, Graz, AUT*



### ABSTRACT

*The paper presents a coupled Flame Tracking – Lagrangian Particle algorithm for simulating turbulent combustion, pollutant formation, and autoignition in enclosures at conditions relevant to IC engines. The Flame Tracking technique implies continuous tracing of the mean reactive surface and application of the laminar/turbulent flame velocity concepts. The Lagrangian Particle method is based on the joint velocity – scalar probability density function approach for simulating reactive mixture autoignition in the preflame zone and pollutant formation in the postflame region. The coupled algorithm is supplemented with the database of tabulated laminar flame velocities as well as reaction rates of fuel oxidation and pollutants (NO, soot, etc.) formation in the wide range of initial temperature, pressure, and equivalence ratio for several premixed hydrocarbon – air compositions. The look-up tables contain information on flammability limits to identify the conditions of flame quenching. Several 2D and 3D computational examples are presented for combustion of propane and n-heptane in enclosures with simple geometries. A possibility of low-temperature preflame autoignition in multiple hot spots has been successfully demonstrated. Space and time resolved dynamics of nitrogen oxide (both prompt and thermal) has been obtained. The coupled algorithm was compared with some conventional approaches and proved to be computationally efficient and to provide less grid dependency of the results.*

**KEY WORDS:** Computational Fluid Dynamics, Combustion Modeling, Preflame Autoignition, Pollutant Formation.

### INTRODUCTION

The objective of any combustion model is to provide correct values of mean reaction rates regardless the combustion mode in a turbulent reactive flow. The mean reaction rate can be obtained provided one knows the reaction kinetics and the local instantaneous fields of temperature and species concentrations. The development of reaction kinetics is the separate task which is independent of combustion modeling. The only relevant issue is the CPU time required for calculating instantaneous reaction rates. This issue can be overcome by applying properly validated short overall reaction mechanisms and/or look-up tables. The local instantaneous fields of temperature and species concentrations are usually not known. Therefore one has to replace this lacking information by a combustion model.

There exist many combustion models both for laminar and turbulent flows. If chemistry is fast as compared to mixing, the Spalding Eddy-Break-Up model can be used (Spalding, 1976). It is simple but has a limited range of validity. There is a whole class of statistical combustion models (based on the formalism of probability density functions) with probabilistic representation of turbulence and its interaction with chemistry (Pope, 1990). Despite many attractive features, this approach is still not capable of operating with complex chemistry due to inadequate CPU requirements. Moreover, such approaches do not resolve different scales in the turbulent flow and their energy content. Instead, all scales are treated indifferently whereas their effect on combustion and flame is different. Nevertheless, these approaches look very promising for treating autoignition problems. The other class of models deals with a flamelet approach (Peters, 1986). In this approach, the instantaneous flame is assumed to consist of localized reactive sheets, which are transported by the flow and wrinkled by turbulent eddies. The flamelet approach is applicable when the characteristic turbulent scales are larger than a typical flame thickness. This condition is satisfied in many practical situations including frontal combustion in piston engines. The flamelet models are usually based on the flame surface density concept or apply probability density functions. One of the most attractive flamelet models is based on the balance equation for the flame surface density. This equation governs the transport of the mean reactive surface by the turbulent flow and includes physical mechanisms responsible for flame surface area production and destruction.

The approach used within this study is also based on considering the flame surface area. However, to speed-up calculations, instead of solving the partial differential equation for the flame surface density, it implies tracing of the mean reactive surface and application of the laminar/turbulent flame velocity concepts.

## FLAME TRACKING METHOD

The approach outlined below will be referred to as the subgrid model of laminar/turbulent combustion. Let us first explain the essence of the model on the example of laminar flame propagation. The flame surface shape and area can be found based on the Huygens principle (Fig. 1): Each elementary portion of the flame surface  $a-b-c-...-i-j-k$  displaces in time (*i*) due to burning of the fresh mixture at local velocity  $u_n$  (normal to the flame surface) and (*ii*) due to convective motion of the mixture at local velocity  $V$  (see segment  $g-h$ ). The local instantaneous velocity  $u_n$  can be taken from the look-up tables including in

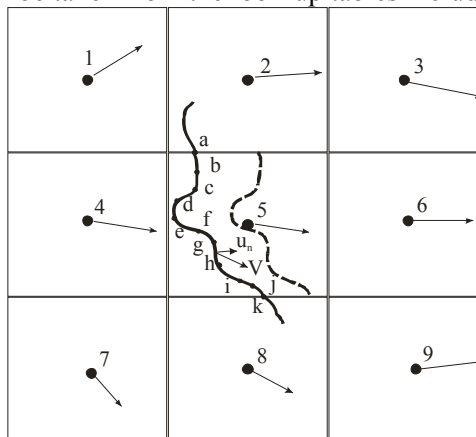


Figure 1: Laminar flame subgrid model: 1 to 9 are the cell centers;  $a-b-c-...-j-k$  is the lumped flame front at previous time step; dashed curve is the new position of the flame front;  $u_n$  is the laminar flame velocity,  $V$  is the interpolated flow velocity vector. The new flame position is found based on the Huygens principles.

general the effects of exhaust gas recirculation (EGR), flame stretching, and flammability limits. The local instantaneous velocity  $V$  can be calculated using a high-order interpolation technique (e. g., using the velocity values in nodes 1 to 9 in Fig. 1). In Fig. 1, the flame surface is represented by straight line segments. In 3D calculations, the flame surface will be represented by connected triangles.

The energy release rate in the computational cell,  $\dot{Q}$ , is composed of two terms: energy release due to frontal combustion,  $\dot{Q}_f$ , and energy release due to volumetric reactions,  $\dot{Q}_v$ . The first term  $\dot{Q}_f$  can be calculated based on the estimated instantaneous flame surface area  $S_n$  and the laminar flame propagation velocity  $u_n$ :

$$\dot{Q}_f = \sum S_{ni} u_{ni} \quad (1)$$

where summation is made over all flame segments (e.g., segment  $g-h$  in Fig. 1) in the cell. The second term  $Q_v$  can be calculated using a particle method (see below).

All pollutants of interest can be sorted as the pollutants formed ( $i$ ) within the flame (e.g., prompt NO) and ( $ii$ ) in the reaction products (e.g., thermal NO, soot, etc.). For calculating the reaction rates for the pollutants of the first sort, one can use the corresponding reaction rates from the laminar-flame look-up tables,  $w_L$ :

$$\dot{W}_L = \sum w_{Li} S_{ni} \quad (2)$$

where summation is again made over all flame segments (e.g., segment  $g-h$  in Fig. 1) in the cell. The formation of the pollutants of the second sort can be calculated using the particle method.

In the turbulent flow field, a pulsating velocity vector distorts the “mean” reactive (flame) surface as shown schematically in Fig. 2 by the thin wrinkled solid curve. The local instantaneous flame wrinkling can be taken into account by proper increasing the normal flame velocity, or in other words, by introducing a concept of local turbulent flame velocity  $u_T$ . The local turbulent flame velocity (e.g., at segment  $g-h$  in Fig. 2) is defined as

$$u_T = u_n S / S_n \quad (3)$$

where  $S$  is the surface area of the wrinkled flame at a given segment and  $S_n$  is the surface area of the equivalent “planar” flame (straight line  $g-h$  in Fig. 2).

The problem now is to find the way of calculating  $u_T$ . In the theory of turbulent combustion, there are many correlations between  $u_T$  and  $u_n$ . One of the classical correlations is Shchelkin formula (Schelkin and Troshin, 1963):

$$u_T \approx u_n \sqrt{1 + u'^2 / u_n^2} \quad (4)$$

where  $u'$  is the local turbulence intensity, related to the turbulent kinetic energy or to pulsating velocity correlations. Instead of Eq. (4) one can use other available correlations for the turbulent flame velocity.

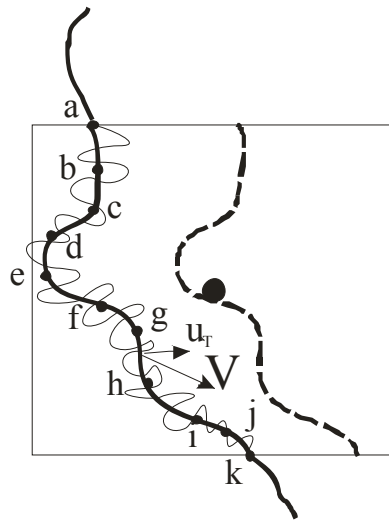


Figure 2: Subgrid model of turbulent combustion: square represents a computational cell with the cell center shown by a large black circle;  $a-b-c\dots-j-k$  is the “mean” flame front at previous time step; thin solid curve is the “instantaneous” flame shape at previous time step; dashed curve is the new position of the “mean” flame front;  $u_T$  is the turbulent flame velocity,  $V$  is the interpolated mean flow velocity vector. The new flame position is found based on the Huygens principle.

One can apply the Huygens principle to model only the “mean” shape of the turbulent flame (solid curve  $a-b-c-d\dots-i-j-k$  in Fig. 2): each elementary portion of the flame surface  $a-b-c\dots-i-j-k$  displaces in time ( $i$ ) due to burning of the fresh mixture at local velocity  $u_T$  (normal to the flame surface) and ( $ii$ ) due to convective motion of the mixture at local velocity  $V$  (see segment  $g-h$ ). The new “mean” flame position is shown by the thick dashed curve in Fig. 2.

The mean energy release rate in the cell,  $Q$ , is composed of two terms: energy release due to frontal combustion,  $Q_f$ , and energy release due to volumetric combustion,  $Q_v$ . The first term  $Q_f$  can be calculated

based on the estimated “mean” flame surface area and the turbulent flame propagation velocity using Eq. (4) (or other correlations). Equation (4) relates the turbulent flame velocity to laminar flame velocity (tabulated) and local turbulence intensity (provided by any model of turbulence). Based on such an equation one can calculate the mean (frontal) energy release rate in the computational cell as the sum

$$\dot{Q}_f = \sum S_{ni} u_{Ti} \quad (5)$$

where index  $i$  relates to the flame surface segment (e.g.  $g-h$  in Fig. 2). In a similar way, one can calculate the mean reaction rates of production/consumption of any reactive species in the turbulent flame. For this purpose, one has to use the look-up tables of the corresponding reaction rate in the laminar flame  $w_{Li}$  and multiply it by the ratio  $u_{Ti} S_{ni} / u_{ni}$  representing the “instantaneous” surface area of the wrinkled laminar flame:

$$\dot{W}_T = \sum w_{Li} u_{Ti} S_{ni} / u_{ni} \quad (6)$$

The second term  $Q_v$  can be calculated using a particle method.

Similar to the laminar combustion case, all pollutants of interest can be sorted as the pollutants formed within the flame (e.g., prompt NO) and in the reaction products (e.g., thermal NO, soot, etc.). For calculating the concentrations of the former, one can use the look-up tables of laminar flame properties and Eq. (6). The concentrations of the latter can be calculated using the particle method.

Thus, the subgrid model of turbulent premixed combustion does not differ much from that of the laminar premixed combustion, except for using  $u_T$  instead of  $u_n$ . Moreover, the formulae like Eq. (4) are asymptotically valid for the subgrid model of laminar combustion (when  $u' \rightarrow 0$ ,  $u_T \rightarrow u_n$ ). It stands to reason that the turbulent combustion model will be also valid for the laminar combustion as a limiting case. This is one of model advantages. This feature will allow using the same model to calculate the initial laminar flame kernel growth from the spark ignition with continuous transition to turbulent combustion. The subgrid combustion model under consideration does not contain tuning parameters (some parameters can be introduced with the equations replacing Eq. (4)). This is the other important model advantage. The additional advantage of the model is that, when coupled with the particle method, it will cover both possible modes of premixed combustion, namely, frontal and volumetric. It is expected that the accuracy of the computational results will be mainly affected by the turbulence model used. The main problem in implementing such a model into a CFD code is the development of an efficient algorithm for “mean” flame-shape tracing inside computational cells. This algorithm should meet the constraints on the flame-front continuity, connectivity, etc., and the constraints on the CPU time consumption.

## PARTICLE METHOD

The particle method allows continuous monitoring of preflame and postflame reactions using the kinetic database (Frolov et al., 1997).

The preflame zone exhibits volumetric reactions of fuel oxidation, formation of intermediate products like alcohols, aldehydes, peroxides, etc. In general, the preflame reactions are inhomogeneous due to inhomogeneous distributions of temperature and main species concentrations. The preflame reactions can result in the localized energy release. For example, low-temperature cool-flame oxidation of  $n$ -alkane fuels can result in the release of up to 10%–15% of the total reaction heat. Thus, in general, two-way coupling approach has to be applied for the preflame reactions, however in some cases one-way coupling is also possible. The direct (and CPU time consuming) way to calculate the volumetric reaction rates is to solve the equations of chemical kinetics in the preflame zone in each computational cell. To shorten the CPU time, one can introduce a certain number of trace Lagrangian particles which will move in the preflame zone according to the local velocity vector. In each particle, the preflame reactions will proceed at the rates determined by its instantaneous temperature and species concentrations. For determining the time and location of preflame autoignition there will be a need in adopting a certain criterion. Such a criterion can be based on the fixed rate of temperature rise in the particle, e.g.,  $10^7$  K/s.

In case of one-way coupling, the ignition delay based on the local preflame temperature and species concentrations is calculated in each particle, while preflame reactions do not affect the flow pattern. When the autoignition criterion is met in one or several particles, new (forced) ignition sites in the preflame zone can be automatically introduced. These ignition sites give birth to new laminar/turbulent flame kernels. The

number of particles in the preflame zone can be much less than the number of computational cells. For keeping the number of particles at a reasonable level, the consistent procedures of particle cloning and clustering should be developed. The preflame particles are traced until the entire geometry is traversed by the flame(s).

The postflame zone exhibits volumetric reactions of residual fuel pyrolysis, oxidation, etc., and pollutants formation. These reactions can influence the flow pattern. Therefore the two-way coupling is usually required. For example, soot formation in fuel-containing combustion products can result in fuel depletion and temperature variation. To take into account possible turbulence–chemistry interaction, a supplementary (coarse) grid for the Particle method can be constructed. Each element of this grid should contain enough particles to represent possible realizations of the turbulent velocity field. Thus, the instantaneous pulsating velocity vector can be modeled using random number generators providing properly normalized random numbers. In each particle, the pollutants are accumulated or depleted at the rates determined by the particle temperature and species concentrations. Each particle has a proper “weight” to ensure the integral balance of mass. The emission indices of pollutants are then calculated by summing over all particles. The corresponding source terms are found, for example, by interpolation from the particles into cell centers.

### KINETIC DATABASE

As was mentioned above, the coupled Flame Tracking – Particle algorithm is supplemented with the database of tabulated laminar flame velocities, prompt NO, etc., as well as the reaction rates of fuel oxidation and pollutants (thermal NO, soot, etc.) formation in the wide range of initial temperature (from 300 to 900 K), pressure (from 1 to 100 atm), equivalence ratio (from very fuel-lean to very fuel-rich mixtures), and EGR (up to 80%) for several premixed hydrocarbon – air compositions (methane, propane, ethanol, n-heptane, etc.). The look-up tables contain information on flammability limits to identify the conditions of flame quenching.

### RESULTS OF TEST CALCULATIONS

The coupled Flame Tracking – Particle method has been developed and implemented into AVL FIRE code. As an example, let us consider the results of the 2D test case with turbulent flame propagation in a channel closed from both ends. Figure 3 shows the computational grid and boundary conditions. The channel was initially filled with the stoichiometric propane – air mixture at the temperature and pressure of 700 K and 4 atm, respectively. The initial flame kernel was assumed to be a circle 1 cm in radius with the center located at 1 cm from the left wall at the symmetry plane. The turbulent flame velocity was modeled by the Shchelkin formula (Eq. (4)). The laminar flame velocity entering Eq. (4) was linearly interpolated using the data of look-up tables for propane. The kinetic parameters used for calculating preflame oxidation were taken from the corresponding look-up tables for propane. Turbulence was modeled by the  $k$ – $\epsilon$  model. In this test case, preflame autoignition was observed in the calculation. Figure 4 shows temporal evolution of temperature and propane mass fraction. As is seen the flame tracking method avoids numerical diffusion of scalars through the flame front: the flame is concentrated inside a single computational cell. At time 38.85 ms (last frame in Fig. 4) preflame autoignition occurs.

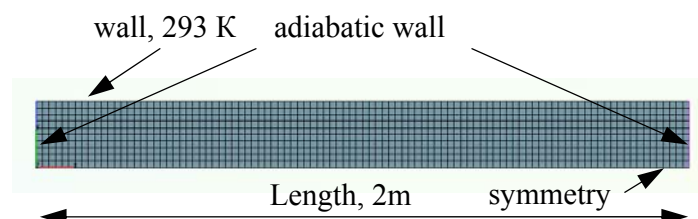


Figure 3: Computational grid and boundary conditions for the test case with flame propagation in a closed channel.

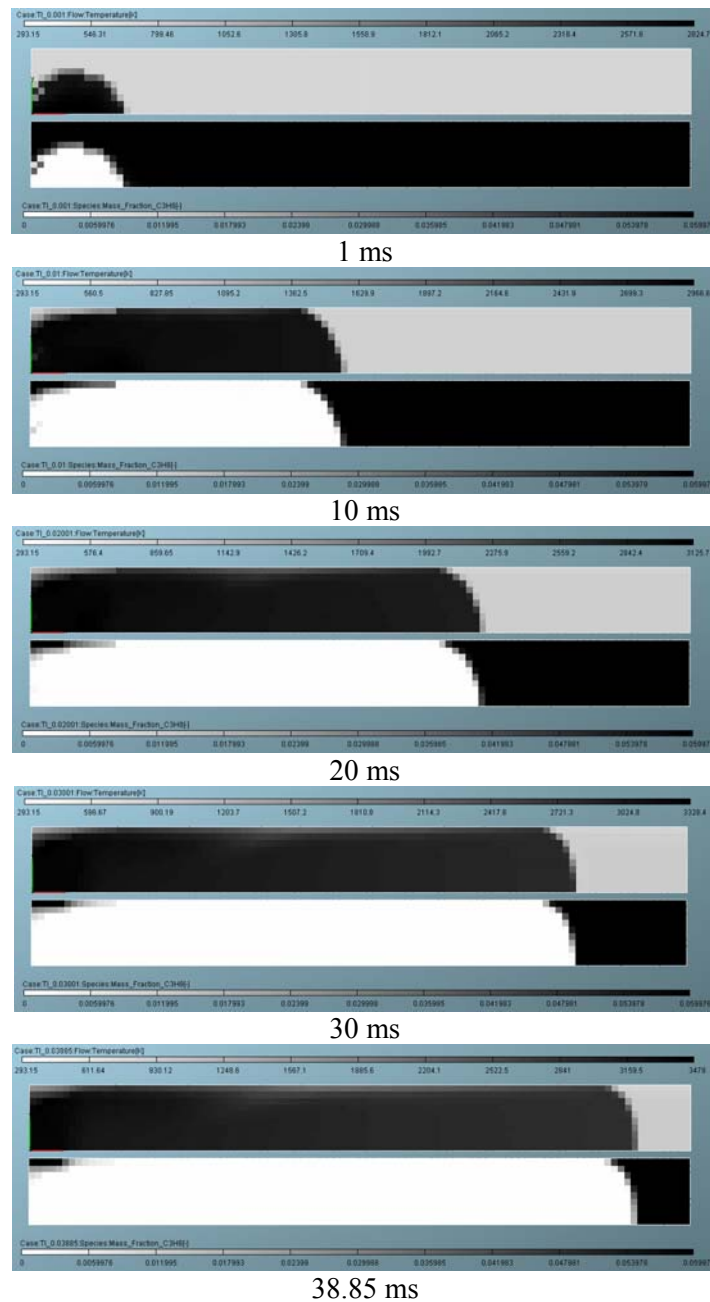


Figure 4: Temporal evolution of temperature (upper snapshots) and propane mass fraction (lower snapshots) in the course of turbulent flame propagation in a closed channel and preflame autoignition.

Figure 5 shows the time history of the distance traveled by the flame. As expected, the flame decelerates in the course of propagation. Figure 6 compares the calculated temperature histories in the computational cell initially located in the preflame zone (dotted curve) and in the notional particle (solid curve) located in this cell. Also shown in Fig. 6 is the time history of propane mass fraction in the notional particle. The autoignition in the notional particles occurs prior to flame arrival to the specified computational cell. The autoignition in the particle is two-stage: at the first (cool flame) stage, the particle temperature increases to about 775 K, whereas at the second stage (hot explosion) the particle temperature sharply increases up to the combustion temperature.

The advantage of the Particle method is that it provides the location of autoignition hot spots. Black spots in Fig. 7 show the computational cells where localized autoignition occurs at two subsequent time steps. At the first time instant, one can see the flame front and several hot spots in the preflame zone. At the second time instant (in  $20 \mu\text{s}$ ) nearly entire preflame zone is autoignited except for the near-wall

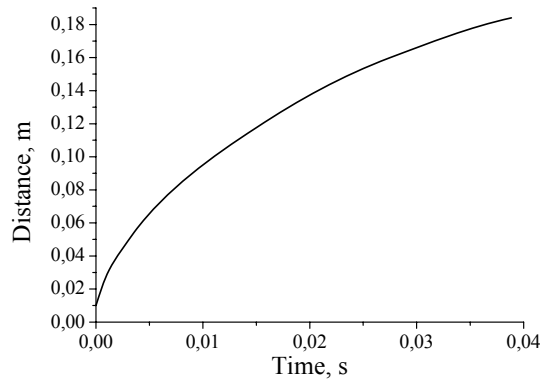


Figure 5: Time history of the distance traveled by the flame in a closed channel in the stoichiometric propane – air mixture at the initial temperature of 700 K and pressure of 4 atm.

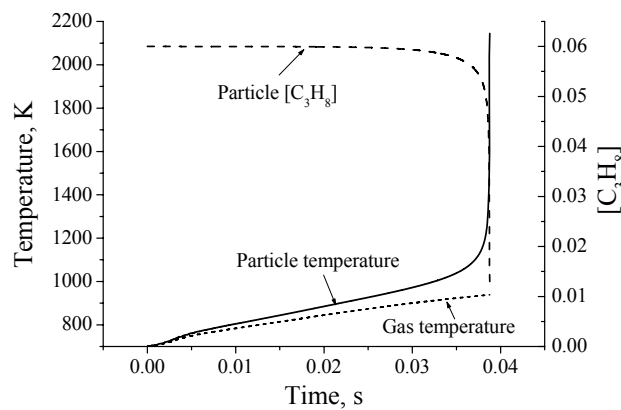


Figure 6: Comparison between calculated temperature histories in the computational cell initially located in the preflame zone (dotted curve) and in the notional particle (solid curve) located in this cell. Dashed curve shows the time history of propane mass fraction in the notional particle. Preflame autoignition occurs at 38.85 ms.

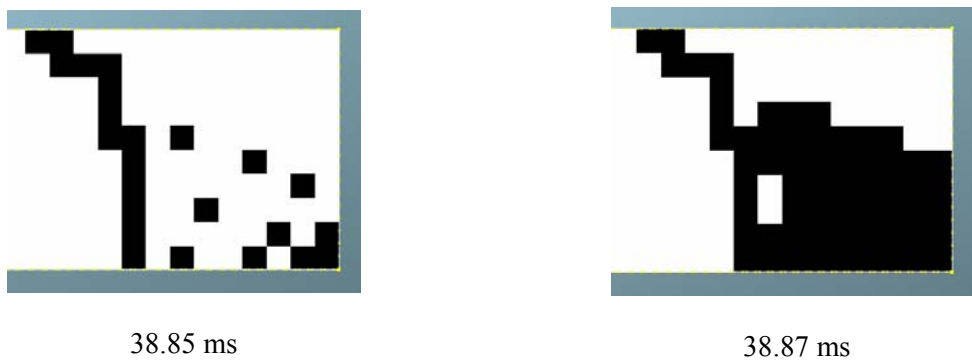


Figure 7: Formation of hot spots in the preflame zone due to autoignition.

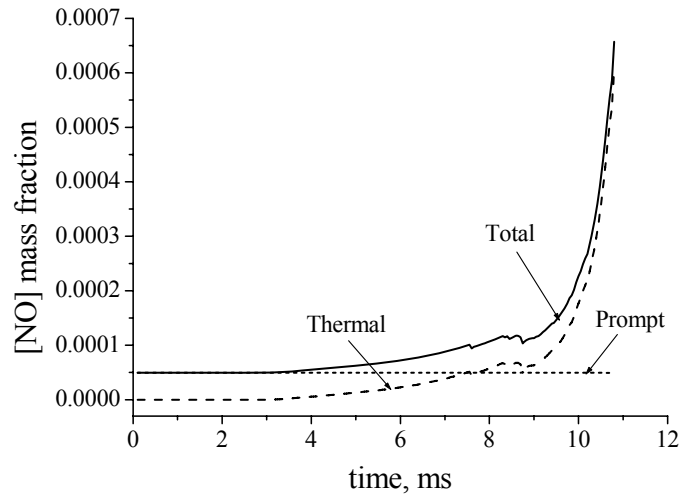


Figure 8: Time history of nitrogen oxide mass fraction during combustion of *n*-heptane – air mixture in a 3D enclosure  $0.14 \times 0.14 \times 0.14$  m.

region of the channel. The near-wall region is affected by the wall due to the isothermal wall boundary condition. Thus, the coupled Flame Tracking – Particle algorithm allows for the spatial and temporal resolution of preflame autoignition which is very important for simulating engine knocking conditions.

Using the same code, 3D calculations in the cubic enclosure  $14 \times 14 \times 14$  cm were also made for the stoichiometric *n*-heptane – air mixture initially at normal atmospheric conditions (293 K and 1 atm) and very low turbulence intensity. As a result of this test case, the time history of NO mass fraction in the enclosure was calculated and plotted in Fig. 8.

In addition, the 3D Flame Tracking – Particle method was tested on its capability of providing spatial and temporal evolution of preflame autoignition. For this purpose, the cubic enclosure  $5 \times 5 \times 5$  cm was initially filled with the stoichiometric *n*-heptane – air mixture at 700 K and 8 atm. In 8 ms after forced ignition in the cube center, preflame autoignition was detected. Figure 9 shows the flame front position at this time instant as well as autoignition hot spots (marked by points).

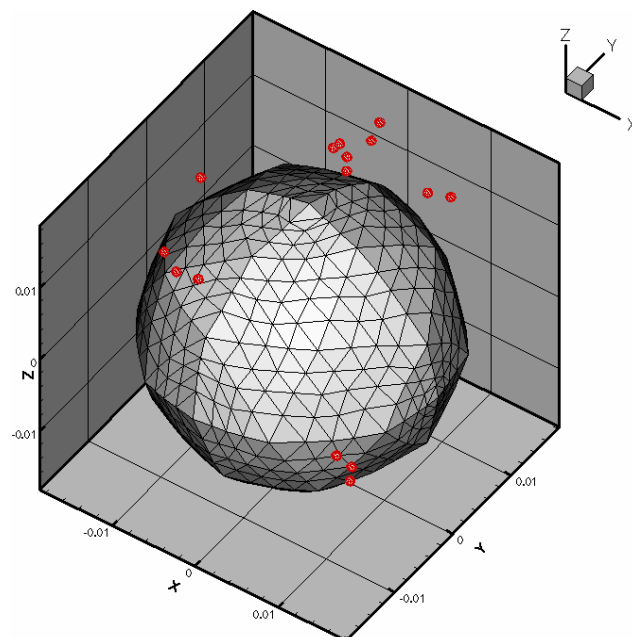


Figure 9: Flame shape at the instant of preflame autoignition. Points show the autoignition sites.

## CONCLUDING REMARKS

A coupled Flame Tracking – Particle method combined with the look-up tables of laminar flame velocities, fuel oxidation, and pollutant formation rates has been developed and implemented into AVL FIRE code. The method is parameter free and very efficient in terms of CPU requirements. It provides spatial and temporal resolution of preflame autoignition sites as well as pollutant (NO, soot, etc.) formation both in the flame front and in the combustion products. The algorithms have been tested for several 2D and 3D flame configurations in enclosures and demonstrated good solution convergence and stability. Further efforts will be directed on the validation of test calculations against available experimental data for IC engine conditions.

## ACKNOWLEDGMENTS

The authors thank Prof. Basevich V. Ya., and Dr. Belyaev A. A. for developing look-up tables. The work was supported by the AVL LIST GmbH and Russian Foundation for Basic Research (grant 08-08-00068).

## REFERENCES

- Frolov, S.M., Basevich, V.Ya., Neuhaus, M.G., Tatschl R., 1997, “A Joint Velocity – Scalar PDF Method for Modeling Premixed and Nonpremixed Combustion”, In: *Advanced Computation and Analysis of Combustion*, edited by G.D. Roy, S.M. Frolov, P. Givi, Moscow, ENAS Publ., 537–561.
- Pope, S. B., 1990, “Computation of Turbulent Combustion: Progress and Challenges”, *Proc. Comb. Inst.*, Vol. 23, 591-612.
- Peters, N., 1986, “Laminar Flamelet Concepts in Turbulent Combustion”, *Proc. Comb. Inst.*, Vol. 21, 1231–1250.
- Spalding, D. B., 1976, “Mathematical Models of Turbulent Flames, a Review”, *Comb. Sci. Techn.*, Vol. 13, 3–25.
- Schelkin, K.I., Troshin, Ya. K., 1963, “Gasdynamics of Combustion”, Moscow, USSR Acad. Sci. Publ.